

Wireless and Batteryless Vibration Testing of Space Structures with Implanted LSI Sensors

J. Mitsugi^{a*}, N. Rajoria^a, Y.Kawakita^b and H.Ichikawa^b

^a Auto-ID Laboratory, Keio University, 5322 Endo Fujisawa, Kanagawa 252-0882, Japan, mitsugi@keio.jp

^b The University of Electronic Communications, 1-5-1 Choufugaoka, Chofu, Tokyo 182-8585, Japan

* Corresponding Author

Abstract

Vibration testing and modal survey of space structures usually afflict labour intensive and delicate sensor attachments and power/signal wire routings not to damage delicate space structures. In this paper, we propose to implant tiny wireless and batteryless sensors to space structures at the time of fabrication to eradicate the power/signal wiring burden for their entire structural lifecycle by providing power to the implanted sensors with radio wave. The vibration data is concurrently collected from multiple sensors as the reflection of radio wave. The mutually interfering reflections are processed in an interrogator to separate the signals to produce a transition matrix. The concurrent and synchronized collection of sensor data is realized by a newly invented wireless access method tailored to low functional sensors, referred to as Multiple Subcarrier Multiple Access (MSMA). In this paper, we outline the theory and challenges of MSMA and report the state of art of the development with experimental results.

Keywords: Modal Survey, Vibration Testing, Wireless Sensor, Software Defined Radio, Passive Backscatter

Acronyms/Abbreviations

- CDMA: Code Division Multiple Access
- CIR: Carrier to Interference Ratio, representing signal quality contaminated with interference.
- EIRP: Equivalent Isotropic Radiation Power, the sum of transmit power and antenna gain
- FDMA: Frequency Division Multiple Access
- MSMA: Multiple Subcarrier Multiple Access
- RFID: Radio Frequency Identification
- RF: Radio Frequency
- RSSI: Received Signal Strength Index, Received signal RF power.
- SDR: Software Defined Radio
- SHM: Structural Health Monitoring
- TDMA: Time Division Multiple Access

1. Introduction

The structural integrity of a space structure has to be qualified through modal survey or vibration testing at several stages in the development. Since attaching accelerometers and routing their wire harnesses demand delicate and time-consuming labour, we often are forced to limit the number of such testing at the minimum.

The purpose of this research is to facilitate the ground testing and even to realize on-orbit testing to check the structural integrity of space structures with wireless and batteryless sensors which are implanted to space structures at the time of fabrication and are used for the entire structural life. The principal challenges of wireless and batteryless vibration testing are the power supply to sensors and the concurrent collection of multiple sensor data streaming concurrently. The latter is essential to

correlate the acceleration measurement and the excitation force to derive the transient matrix of the structure in the form of Bode or Nyquist diagrams.

The industrial needs to take preemptive action to prevent fatal accidents by continuously monitoring the integrity of structures are, in general, categorized as Structural Health Monitoring (SHM). With the advancement of LSI technology and wireless communications, SHM is an active research field not only in aerospace industry but also in civil structures[1]-[6]. Noel et.al [7] provides a good survey on the wireless SHM. The survey reveals that the tight sensor synchronization, less than 120 micro second with up to 70 sensors is one of the challenges under common vibration environment where major eigen frequencies reside below 100 Hz.

Wireless and batteryless sensing can be realized by using the passive backscatter technology. The advanced processing and rectifying technology enable less than 10 uA with low voltage CMOS power consumption to bidirectional communication between multiple sensors and an interrogator[8][9]. The sensitivity of commercial wireless and batteryless chip reaches -20 dBm [10], which is equivalent to the 10 uA power level. It should be noted that a special wireless communication method shall be used in a passive backscatter system because of the need of continuous powering to the sensors and the poor signal processing capability of sensors.

The time synchronicity in wireless communications is usually secured by an access method which separates radio resources such as time, frequency or code namely TDMA, FDMA and CDMA, respectively. However, those existing access methods cannot be directly applied

to a passive backscatter system because the burst transmission, the narrow band channel filter and the transmission power control required to accomplish TDMA, FDMA and CDMA, respectively demand a signal processing capability and an autonomous transmission capability which are too high or impracticable for passive backscatter sensors. Existing passive RFID system multiple access method [11], basically a TDMA without burst transmission, cannot meet the synchronicity requirement too.

The authors have been developing a multiple access method referred to as Multiple Subcarrier Multiple Access (MSMA) tailored to passive backscatter system for wireless SHM of space structures and civil structures[12]-[16]. An image of using MSMA in an airplane health monitoring is shown in Figure 1 where the aircraft is supposedly equipped with many implanted sensors. Since we can perform a modal survey swiftly with many sensing points at a very low cost without harnessing any wires, even a local structural damage or failure can be detected by comparing the past and similar measurements.

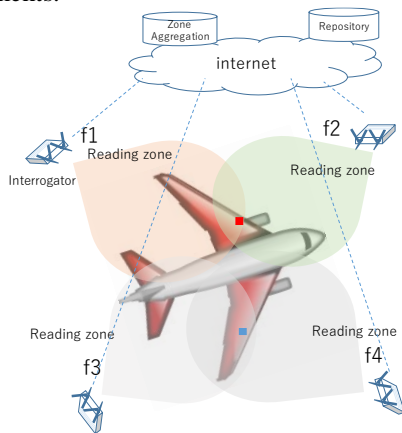


Figure 1 Use case of MSMA based SHM of an aircraft

In this paper, we outline the theory and challenges of MSMA and report the state-of-art developments with experimental performance evaluations.

The rest of the paper is organized as follows. Section 2. overviews the theory of MSMA and its challenges. Section 3. explains our prototype implementation of MSMA. Section 4. reports the state of art performance of prototype system. Section 5. concludes the paper.

2. Theory and challenges of MSMA

The principal components in an MSMA system are sensor tags, an interrogator and a signal processing server as shown in Figure 2.

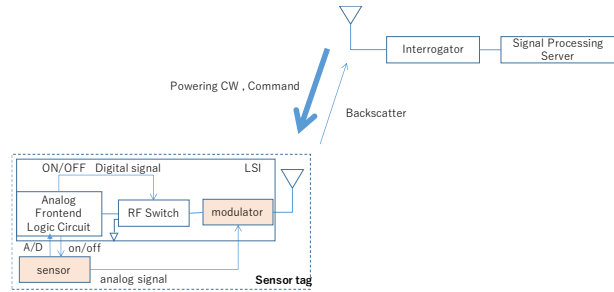


Figure 2 Principal components in MSMA

Each sensor tag is furnished with a sensor. The type of sensor is chosen based on the application. In vibration and modal testing of space structures, accelerometer should be the choice. Low power MEMS accelerometers are available in the market. Since MEMS sensor and RF LSI cannot be produced with single process, a sensor tag is expected to be realized either a bare LSI or an IC package housing multiple chips insides as shown in Figure 3.

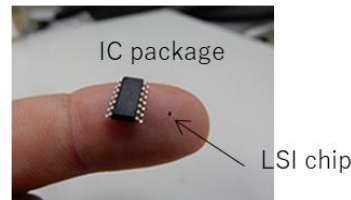


Figure 3 Expected production images of sensor tag

Sensor data is either analog or digital modulated onto the backscatter by using a modulator in analog modulation and an RF switch in digital modulation. In the case of modal survey, the required sensor data is not a single packet but data streaming. To produce a sensor data streaming, each RF tag is given a dedicated subcarrier frequency channel by the interrogator and backscatters at the channel. A subcarrier can be easily produced by superposing a constant on/off produced by an embedded RF switch onto the sensor data but doing so inevitably produces harmonics as shown in Figure 4.

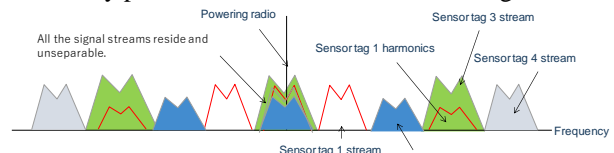


Figure 4 Frequency spectrum of multiple sensor tag backscatters

The harmonic components are generated at the odd multiples of the principal subcarrier channel theoretically. Taking advantage of this theory, the signal processing server produces replicas of harmonics from a principal subcarrier and rejects the interference successively. A simple mathematical representation of a four sensor tag system is as Eq. 1 where R_i represents the i -th channel received signal and T_j represents the j -th sensor tag transmission at the j -th channel.

$$\begin{matrix} \text{Received signals} & & \text{Transmitted signals} \\ \left\{ \begin{matrix} R_1 \\ R_2 \\ R_3 \\ R_4 \end{matrix} \right\} = \begin{bmatrix} 1 & 0 & 0 & 0 \\ 0 & 1 & 0 & 0 \\ 1/3 & 0 & 1 & 0 \\ 0 & 0 & 0 & 1 \end{bmatrix} & & \left\{ \begin{matrix} T_1 \\ T_2 \\ T_3 \\ T_4 \end{matrix} \right\} \end{matrix} \quad (1)$$

harmonics

Because of the lower triangle matrix nature, we can reconstruct the transmitted signals T_j from the received signals. In practice, the replica generation and harmonics rejection is a little more complex to accommodate phase and group delays but the above generalization provides a comprehensive overview of the method.

The technical challenges to make MSMA work are majorly the following three.

(1) **Interference rejection:** Since MSMA uses the passive backscatter as the media of sensor data streaming, the signal quality is inherently poor. In order to secure large separation between symbols in the backscatter signal, it is a common practice to apply a high pass filter at the ingress of the interrogator to maximize the symbol separations. In return, however, we need to produce harmonics replicas from a zero cross signals.

(2) **Optimized frequency channel allocation:** Since the received power from a sensor tag is dictated by the distance to the sensor tag, the bandwidth of the sensor tag and the propagation channel, we need to allocate the frequency channels to maximize the frequency usage efficiency. A careless frequency channel allocation leads to a poor carrier to interference ratio (CIR) yielding erroneous demodulated signals.

(3) **Interrogation zone aggregation:** Because of the backscatter principle, the interrogation zone of MSMA is inherently smaller than that of active wireless sensor system. For large structure applications, interrogation zone aggregation should be developed.

The complete sensor data collection flow of MSMA is as follows.

- (1) Firstly, an interrogator inventories the sensor tags in its RF view field. Unique ID of each sensor RF tags with RSSI and phase are collected using an existing RFID protocol such as [11].
- (2) Base on the RSSI and phase and other information, the interrogator and signal processing server determine the frequency channel.
- (3) The interrogator commands the sensor tags to start data streaming. Simultaneously, the signal processing server instructs the modal excitation system to the vibration testing system.
- (4) The signal processing server collects sensor data streaming and applies the interference rejection by producing and subtracting backscatter replica. To this end, we can establish a transition matrix between the excitation force and the amplitude and

phase responses at many places of the target structure.

- (5) If multiple interrogations are used, the component transition matrices are coherently aggregated to obtain the transition matrix of integrated structure.

The whole procedure is summarized in Figure 5.

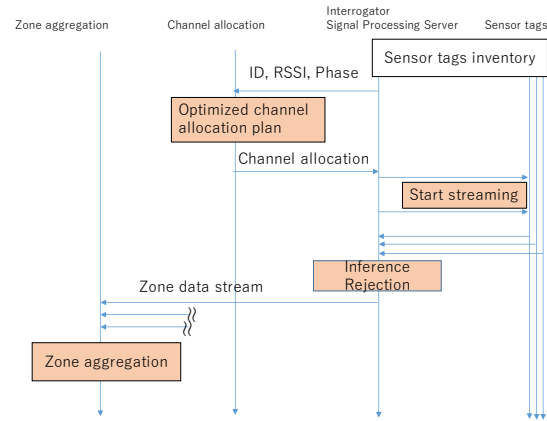


Figure 5 MSMA processing flow

In the following subsections, our technical developments on the three challenges are explained.

2.1 Interference rejection

The problem to generate harmonics is the zero crossing signal whose IQ trajectory is shown in Figure 6 where ω_s denotes the subcarrier angular velocity and ψ is the phase offset derived from the sum of the distance between sensor tag and interrogator and the modulated signal.

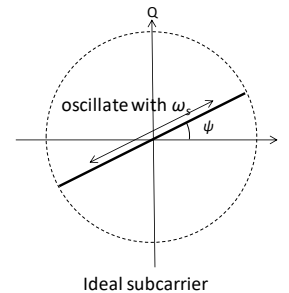


Figure 6 Backscatter signal after DC component subtraction forms a zero crossing signal

We first apply Hilbert transformation to produce an analytic signal which is orthogonal to the physical signal and has the temporal amplitude with which the physical signal can rotate the IQ plane. Hilbert transformation is like generating a cosine wave from a given temporal sine wave. The combined physical and analytic signals, thus, rotates around zero in the IQ plane. By applying a numerical phase lock loop to obtain harmonics and apply the corresponding amplitude decay, we can produce replica from the combined signal as shown in Figure 7. In the figure, the third harmonics is depicted from the combined signal as an example. Analytic signal gives us

the information on the subcarrier phase delay Φ_s , which is concealed in the zero crossing signal.

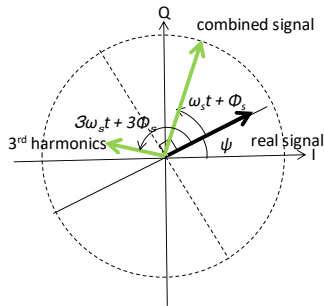


Figure 7 Third harmonics generation with analytic signal after Hilbert transformation.

The generated replica shall be converted to a zero crossing signal. For this purpose, we invent an inverse Hilbert transformation by projecting the replica onto the ψ angle rotated axis. This inverse Hilbert transformation is illustrated in Figure 8. The detail derivation of the interference rejection method can be found in [13][15].

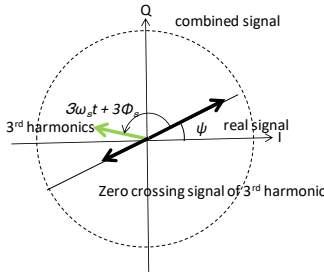


Figure 8 Harmonic replica is generated by projecting back to the original phase.

Different from the existing collided signal separation methods such as [17][18][19], the interference rejection in MSMA is applied in the analog wave shape. Thus, it is independent from the modulation scheme choice.

2.2 Optimized frequency channel allocation

Because harmonics are produced at odd multiples of subcarrier frequency channel, channels near to the powering frequency, referred to as near channels, are influential to produce interference. Therefore, allocating near channels to far sensor tags produces less total interference. Similarly, sensor tags demanding narrow bandwidth is influential compared with wide bandwidth sensor tags. Allocating near subcarriers to wide bandwidth sensor tag is, therefore, a good strategy too.

The problematic situation is the indecision cases where we prioritize either a far and narrow bandwidth sensor tag or a near and wide bandwidth sensor tag.

Since this is a permutation problem, examining every possibility is impracticable particularly when the number of sensor tags are large.

We derive a heuristic performance index referred to as “total contamination power” to prioritize the channel allocation. The principle is quite straight forward. If we

have an indecision pair of sensor tags, we calculate the sum of the principal subcarrier and harmonics power of each sensor tag in the available band and use this as the performance index. We prioritize the sensor tag which produce less total contamination power.

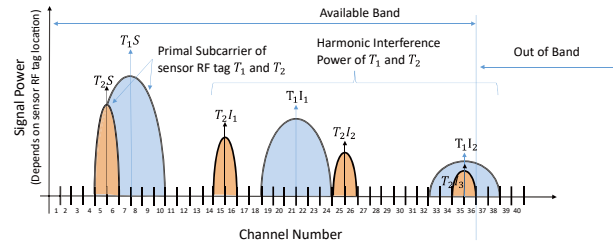


Figure 9 Example comparison of a indecision case with total contamination power

Detailed derivation of the optimized frequency channel allocation can be found in [13][14][16].

2.3 Interrogation zone aggregation

After the establishment of the component transition matrices, the whole structural response can be derived with the traditional component mode synthesis. But because of the autonomy in the component MSMA systems, we may adjust the frame synchronization error and the time delay to complete the signal processing for the coherency of the aggregation [19].

3. Prototype MSMA system

In parallel with the theoretical development, we have been developing a prototype MSMA system.

As the interrogator and signal processing server, we use a software defined radio platform USRP2952R and LabVIEW communication 2.0 running on Core i7 3.6GHz Windows 7 PC.

Since the design and fabrication of sensor tag LSI demands a large investment and is too early, we currently develop PCB prototypes to examine the elemental technology and to reveal the practicality of the proposal.

3.1 Interrogator and signal processing server

For now, we only implement a signal processing server with the function to send powering continuous radio wave because the interrogator part does not require new development.

The signal processing server comprises a NI USRP 2952R and a PC which runs LabVIEW communication 2.0 as the toolchain for the signal processing. Since the maximum transmission power of NI USRP 2952R is 20dBm we use a 40dB power amplifier R&K A00110-4049-R to obtain 30dBm power with -10dBm output of the USRP. The 30dBm output power is limited by our radio station license. We use 6dBi antenna both in transmission and receiving.

The outline of signal processing diagram in LabVIEW taking a nine subcarrier system as an example is shown

in Figure 10. In the figure, DEM denotes a demodulator. As it might be noted, the number of interfered channel is rather limited. As the harmonic decreases as reciprocal to the harmonics order, only the first and second harmonics replica need to be generated in practice.

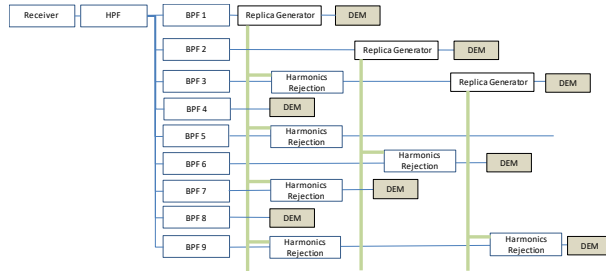


Figure 10 Outline of signal processing in LabVIEW communications of a 9 subcarrier system

3.2 Sensor tag

The first prototype we made comprises an Atmel ATtiny24 MCU as shown in Figure 11.



Figure 11 MSMA sensor tag first prototype

The prototype is exclusively battery powered and the total power consumption is 3mA at 3 volt when we use 8 MHz internal clock.

The second prototype has a batteryless mode in addition to a battery mode using Farsens ANDY 100 power harvester. The use of low power consumption Atmel SAML21 and a digital accelerometer Analog Devices ADXL362 enables batteryless operation at about 1m.

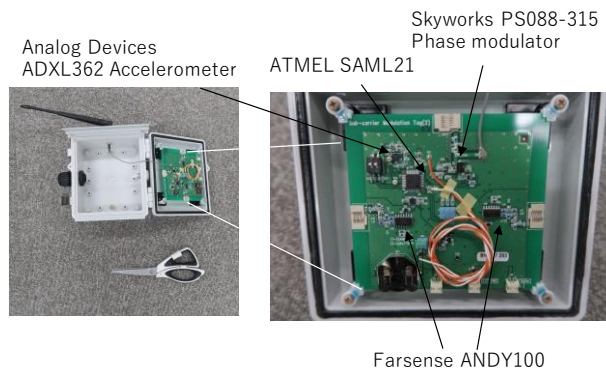


Figure 12 MSMA sensor tag second prototype

The power budget with respect to the clock of the second prototype is shown in Figure 13.

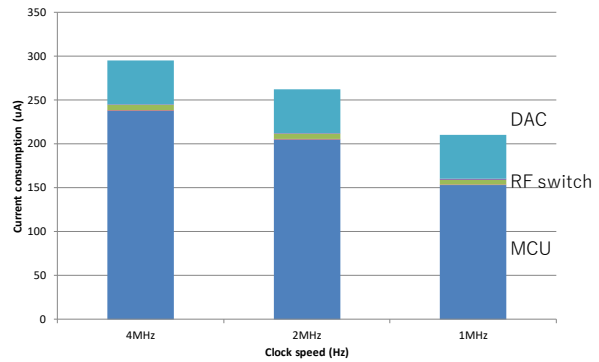


Figure 13 Power budget of the second prototype sensor tag

As we mention earlier in this manuscript, the power consumption can be drastically reduced to the level of less than 10 μ A with existing process technology by fabricating ASIC, which is our next development.

In the second prototype, the prototype firmware is modified to accommodate an external sensor with the embedded A/D converter in SAML21 MCU. The embedded accelerometer ADXL362 is low power and sufficient for modal testing but is not sufficiently sensitive to detect a weak acceleration of 10 milli-g level. Such weak acceleration measurement is demanded in civil structure monitoring, specifically, bridge measurements. The water proof housing of the second prototype is required to perform an out-door wireless measurement of bridge in the fall of 2017. To secure the interrogation distance and provide power to the external sensor, we use the battery mode in the test.

4. Performance evaluation

4.1 Interference rejection

The fundamental performance of interference rejection method is evaluated with a prototype tag and numerical simulation with MATLAB/Simulink. In this test, the sensor tag and the interrogator is connected with a coaxial cable and Carrier to Interference Ratio (CIR) is adjusted by an attenuator. The signal is analog modulated and the auto-correlation between the original and recovered signal shapes is measured. The result is shown in Figure 14.

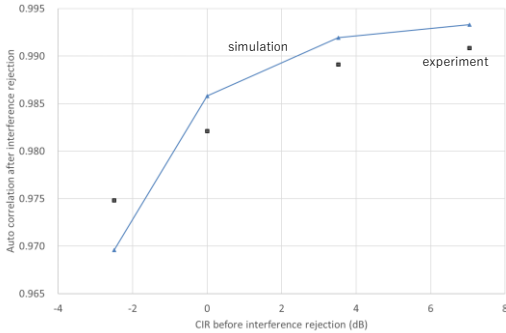


Figure 14 Contribution of the interference rejection

It is shown that even CIR = 0dB environment, which is the worst condition after the optimized frequency channel allocation, the interference rejection recovers the original wave shape with less than 2% error.

In wireless environment, the contribution of interference rejection is degraded because of the unavoidable frequency selective fading. Figure 15 is an example of such performance degradation in in-door propagation environment. The phase and amplitude of the principal subcarrier are not preserved perfectly in the harmonics in the real world propagation, which degrades the replica accuracy. However, we still can secure about 15 dB CIR enhancement with the interference rejection.

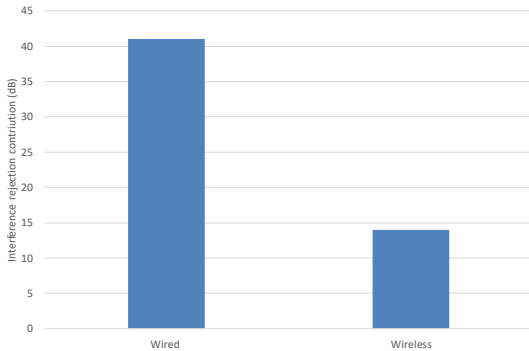


Figure 15 Interference rejection contribution is degraded in wireless environment

4.2 Modal analysis

We experimentally examine the accuracy of modal analysis using three MSMA sensor tags on an aluminium scale. The three subcarrier frequency channels are chosen 10 kHz (ch 1), 30 kHz (ch 3) and 90 kHz (ch 9). The frequency allocation provides the worst interference case for three sensor tags, particularly 90 kHz sensor tag receives interferences from the other two sensor tags. The three sensor tags receive and reflect the radio wave through SMA cable or free space propagation in our laboratory. Experimental setup is shown in Figure 16. The modal sweep is done with an IMV vibration test suit. As a reference, we install three Endevco wired accelerometers besides each sensor tag.

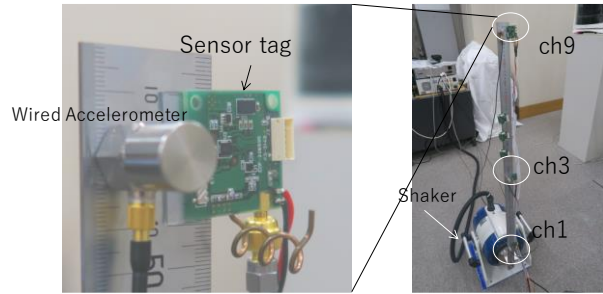


Figure 16 Experimental setup of modal survey

Vibration mode at 100 Hz excitation before and after interface rejection in the SMA cable configuration is shown in Figure 17.

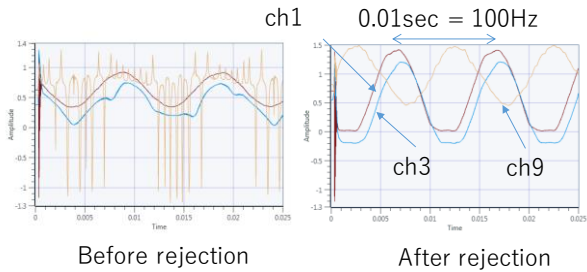


Figure 17 Modal shape before and after interference rejection (SMA cable configuration)

The large fluctuation caused particularly on 90 kHz sensor tag before the rejection is thoroughly rejected with our interference rejection method. In the free space propagation environment, the signals are contaminated with noise. But the interference rejection successfully separate the three signals as shown in Figure 18.

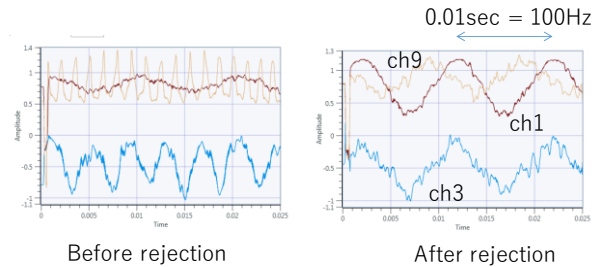


Figure 18 Modal shape before and after interference rejection (indoor propagation).

The responses of wired sensors and MSMA sensor tags are compared to see if the amplitude and phase are properly recovered with MSMA as in Figure 19.

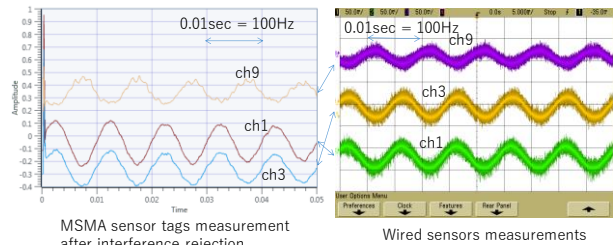


Figure 19 Comparison with wired sensor and MSMA sensor tags measurements

Ch 1 and Ch 3 are almost coherent both in wired and MSMA measurements. Ch 9 is in the opposite phase and the amplitude is about half of Ch 1 and Ch 3. This characteristics is also clearly shown in MSMA measurement too. It should be also noted that the three channels are completely synchronized.

4.3 Reading distance

The reading distance of the second prototype is measured in an outdoor propagation environment. The setup is shown in Figure 20.



Signal processing server side view from the prototype sensor tag

Figure 20 Reading distance measurement

In this case, we employ a digital modulation since analog modulation is vulnerable to environmental phase error which is unavoidable in out-door settings. We use a coin battery in the sensor tag in this experiment.

For the bit error measurement purpose, a fixed bit pattern is generated and transferred from the sensor tag to the signal processing server. The transmission EIRP is 36 dBm. The result is shown in Figure 21. Since BER around 10^{-3} and 10^{-4} are commonplace in general backscatter communication systems[21], less than 20m reading distance seems practicable.

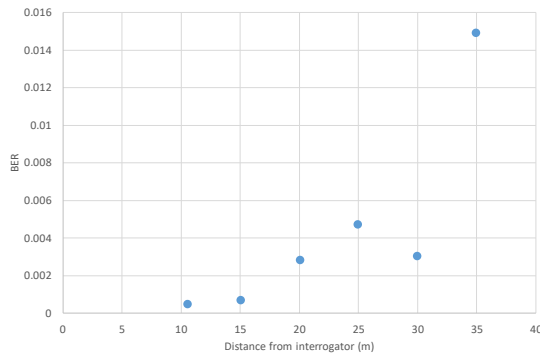


Figure 21 BER measurement with prototype sensor tag

4.4 Optimized frequency channel allocation

CIR before and after the optimized frequency channel allocation based on the contamination power with fifty sensor tags is simulated with MATLAB and is shown in Figure 22.

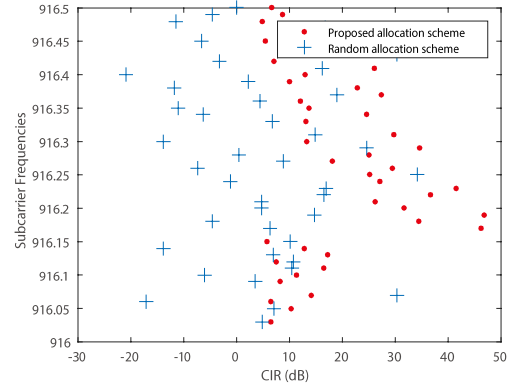


Figure 22 The optimized frequency channel allocation successfully improves the entire CIR.

The results obtained with the total contamination power is compared with the true optimized allocation computed with a brute force trial for eight sensor tags to confirm the obtained allocation is nearly equal to the optimized solution. The order of computations required to reach the optimized solution with the brute force method and the proposal are compared in Figure 23. While the order of computations required in the brute force method is $O(n!)$, that of the proposal is only $O(n^2)$. We can significantly reduce computation time to find an optimized channel allocation in MSMA.

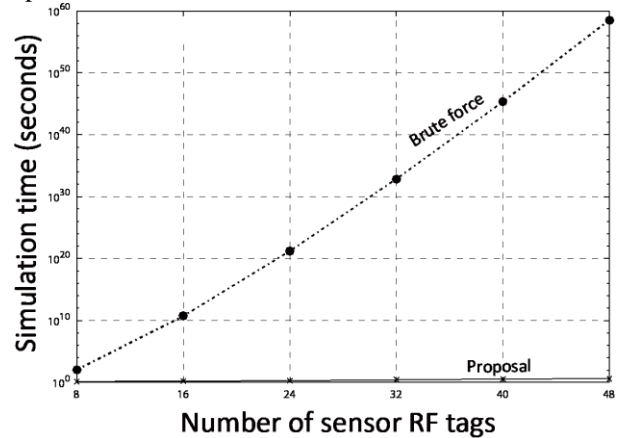


Figure 23 Computation time required in Brute force (estimated) and the proposal

5. Conclusions

Wireless and batteryless sensing in structural health monitoring (SHM) is promising yet challenging because of the requirement on the sensor data synchronicity. Multiple Subcarrier Multiple Access (MSMA) proposed in this paper employs the passive backscatter technology extensively used in RFID and radar and features the specialized signal processing to separate the collided signal using the physical characteristics of harmonics. The synchronization error is virtually zero for 70 sensors in modal survey purposes where the maximum frequency is 100Hz. The current prototype implementation realizes

a batteryless mode within 1 meter distance and still requires a battery for long range sensing and high sensitivity sensing. The batteryless and long range measurement can be realized by fabricating ASIC which is our next research target.

Acknowledgements

This research is supported by Ministry of Internal Affairs and Communications, JAPAN/SCOPE #155003007.

References

- [1] Adee,S., Wireless Sensors That Live Forever, IEEE Spectrum, Jan. 29, (2010), pp.14-14.
- [2] Wilson,W.,C., Atkinson,G.,M., “Passive Wireless Sensor Applications for NASA’s Extreme Aeronautical Environments, IEEE Sensors Journal , Vol.14, no.11, November, (2014), pp.3745-3753.
- [3] George,S.,E., Bocko,M., Nickerson,G.,W., Evaluation of a vibration powered wireless temperature sensor for health monitoring, IEEE Aerospace Conference, (2005), pp.3775-3781.
- [4] Akhond,M.,R., Talevski,A., Cho,T.,H.,Prototype Design and Analysis of Wireless Vibration Sensor, International Conference on Broadband, Wireless Computing, Communication and Applications, (2010), pp.818- 823.
- [5] Xu, N., Rangwala, S., Chintalapudi, K. K., Ganesan, D., Broad, A., Govindan, R., & Estrin, D., “A wireless sensor network for structural monitoring,” Proceedings of the 2nd international conference on Embedded networked sensor systems, Baltimore, MD, USA, (2004). pp.13-24
- [6] Wang, P., Yan, Y., Tian, G. Y., Bouzid, O., Ding, Z., “Investigation of wireless sensor networks for structural health monitoring”. Journal of Sensors, Article ID 156329, (2012).
- [7] A.B.Noel, A. Abdaoui, T.Elfouly, M.H.Ahmed, A.Badawy and M.Shehara. “Structural Health Monitoring using Wireless Sensor Networks: A Comprehensive Survey”, IEEE Communications Survey, Issue 99, (2017) early access.
- [8] Yeager,D, et.al.,”A 9 uA addressable Gen2 Sensor Tag for Biosignal Acquisition”, IEEE Journal of Solid-State Circuits, vol.45, no.10, (2010), pp.2198-2209.
- [9] Okada,H, et.al.,”Development of Custom CMOS LSI for Ultra-Low Power Wireless Sensor Node in Health Monitoring Systems”, IEEE Sensors, (2011), pp.28-31.
- [10] Impinj, Monza 5 Tag Chip Datasheet, <https://support.impinj.com/hc/en-us/articles/202756948-Monza-5-Tag-Chip-Datasheet>.
- [11] ISO/IEC 18000-6, Information Technology - Radio frequency identification for item management- , Part 6 Parameters for air interface communications at 860 MHz to 960 MHz, (2010).
- [12] Igarashi,Y., Sato,Y., Kawakita,Y., Misugi,J., Ichikawa,H., “A Feasibility Study on Simultaneous Data Collection from Multiple Sensor RF Tags with Multiple Subcarriers”, IEEE RFID 2014, April 8-10, (2014)
- [13] Rajoria, N, “Multi-Carrier Backscatter Communication System for Concurrent Wireless and Batteryless Sensing”, Ph.D Dissertation, Keio University, Graduate School of Media and Governance, (2017).
- [14] Rajoria, N., Igarashi,Y., Mitsugi,J., Kawakita,Y., Ichikawa,H., “Comparative analysis on channel allocation schemes in multiple subcarrier passive communication system.” IEICE Transactions on Communications 98, no. 9 (2015): 1777-1784.
- [15] Rajoria,N., Igarashi,Y., Mitsugi,J., Kawakita,Y., Ichikawa,H., “Concurrent Backscatter Streaming from Batteryless and Wireless Sensor Tags with Multiple Subcarrier Multiple Access”, to appear in IEICE Transactions on Communications Vol.E100-B, no.12, Dec.(2017)
- [16] Rajoria,N., Kamei,H., Mitsugi,J., Kawakita,Y., Ichikawa,H., “Performance Evaluation of Variable Bandwidth Channel Allocation Scheme in Multiple Subcarrier Multiple Access”, to appear in IEICE Transactions on Communications Vol.E101-B,No.2.,Feb. (2018).
- [17] Hu,P., Zhang,P., Ganesan,D., “Laissez-Faire: Fully Asymmetric Backscatter Communication”, ACM Sigcomm ‘15, (2015), pp.255–267.
- [18] Shen,D., Woo,G., Reed,D., Lippman,A., Wang,J., “Separation of multiple passive RFID signals using Software Defined Radio”, IEEE RFID, (2009), pp.139–146.
- [19] Wang,Z., Bouwens,F., Vullers,R., Petre,F., Energy-autonomous wireless vibration sensor for condition-based maintenance of machinery, IEEE Sensors, (2011), pp.790-793.
- [20] Yohei Nakano, Tatsuki Fujiwara, Jin Mitsugi, Yuusuke Kawakita, Haruhisa Ichikawa, “Influence by Zone Partition on Large Scale Structure Monitoring Using Wireless and Batteryless Sensors”, IWSSS2016, pp269-270, (2016).
- [21] Bea,J.,H., Choi,W., Park,C.,W., Pyo, C.,S, Kim K.,T., “Design of Reader Baseband Receiver Structure for Demodulating Backscattered Tag Signal in a Passive RFID Environment”, ETRI Journal, Vol.34, No.2, April, (2012), pp.147-158